Draft version May 9, 2022
Typeset using LaTeX default style in AASTeX63

Asteroseismology of a Double mode High-amplitude δ Scuti Star TIC 448892817

Chenglong Lv[1,2] and Ali Esamdin[1,2]

[1]Xinjiang Astronomical Observatory, Chinese Academy of Sciences, Urumqi, Xinjiang 830011, People's Republic of China
[2]School of Astronomy and Space Science, University of Chinese Academy of Sciences, Beijing 100049, People's Republic of China

ABSTRACT

We propose that TIC 448892817 is a double-mode high-amplitude δ Scuti star (HADS). The radial modes detected in this star provide a unique opportunity to exploit asteroseismic techniques up to their limits. Detailed frequency analysis is given for the light curve from the TESS mission, and 30 significant frequencies are detected, while two of them are independent frequencies, i.e. F0 = 13.43538(2) d^{-1}, F1 = 17.27007(4) d^{-1}. The ratio of f_1 / f_2 is measured to be 0.778, suggesting that this target is a high amplitude double-mode δ Scuti star. Nearly all the light variation is due to these two modes and their combination frequencies, but several other frequencies of very low amplitude are also present. The stellar evolutionary models were constructed with different mass M and metallicity Z using MESA. The frequency ratio f_1/f_2 obtained by the model is a little smaller than those obtained by observation. It might be caused by the rotation of the star. The parameters obtained from the model agree well with the results given by previous as well as by the spectra. The best model shows that TIC 448892817 is close to entering the first turn-off of the main sequence. In order to accurately determine the effective temperature and metallicities, thus further narrowing the parameter space of this star, we suggest high-resolution spectra is highly desired in the future.

Keywords: asteroseismology – stars: oscillations – stars: variables: δ Scuti – stars: variables: HADS – stars: individual: KIC 448892817

1. INTRODUCTION

A useful task for diagnosing the physical structure of pulsating stars is asteroseismology (e.g. Brown & Gilliland 1994; Dupret et al. 2004; Aerts et al. 2010; Catelan & Smith 2015; García & Ballot 2019; Daszyńska-Daszkiewicz et al. 2020). During the last years, as a number of missions have received high-resolution data (such as the Microvariability and Oscillations of STars (Walker et al. 2003), Convection, Rotation, and planetary Transits (Auvergne et al. 2009), and *Kepler* (e.g. Gilliland et al. 2010; Koch et al. 2010)), so asteroseismology have been extensively studied (e.g. Yu et al. 2018; Bowman et al. 2021; Aerts 2021; Mombarg et al. 2021; Stello et al. 2022). More recently, *TESS* surveys the most (~85%) sky within the 26 sectors during two years of the primary mission (Ricker et al. 2015) and contributed high-quality photometric light curves of nearby stars (e.g. Campante et al. 2016; Huber et al. 2019). Utilizing such a high-quality database for research will make a significant contribution to the development of asteroseismology as well as stellar structure and evolution.

The δ Scuti star overlay in the HR diagram is roughly divided into two parameter space types, one for the transition region from slowly-rotating low-mass stars with radiative cores and thick convective envelopes ($M \leq 1.5$ $M_\odot$) and the other for rapidly-rotating intermediate mass stars with convective cores and predominantly radiative envelopes ($M \geq 2.5$ $M_\odot$). Such variations in the structure of stars allow the exploration of many different aspects of physics, including pulsation, rotation, magnetic fields and chemical peculiarities (e.g. Murphy et al. 2015; Saio et al. 2015; Chen et al. 2019; Thomson-Paressant et al. 2021; Bowman et al. 2021). Therefore the investigation of δ Scuti is extremely important for testing stellar evolution models. Many pulsation frequencies can be detected in δ Scuti stars, which exist in different pulsation modes. The pulsation modes is mainly in radial and non-radial (e.g. Breger 2000; Uytterhoeven et al. 2011) and are typically excited in the κ mechanism (e.g. Breger 2000; Aerts et al. 2010), these pulsation modes are generally identified as low radial-order (n) low-degree (l) pressure (p) modes (e.g. Viskum et al. 1998; Aerts et al. 2010; Uytterhoeven et al. 2011; Chen et al. 2019). The δ Scuti stars also exist in binary systems (e.g. Chen et al. 2019; Lv et al. 2021), and more precise stellar parameters are obtained by comparing the results of the binary orbital parameters with the results of the steroseismology analysis. Thus, these targets are excellent samples for asteroseismic study, as they could improve our understanding of stellar structure and evolution (e.g. Guo et al. 2019; Murphy et al. 2020; Miszuda et al. 2021).

High-amplitude δ Scuti stars (HADS) are a subclass of δ Scuti stars, which are typically slow rotators with $v \sin i < 30$ km s^{-1}, pulsation periods between 1 and 6 h, and peak-to-peak light amplitudes above 0.3 mag (McNamara 2000). Prior to the release of high-precision space data, the detected HADS usually had only one or two radial pulsation modes of the fundamental and/or first overtone mode (e.g. Yang et al. 2012; Niu et al. 2017; Xue et al. 2018; Yang et al. 2018). The high photometric accuracy of observations thanks to space telescopes in recent decades, especially in *Kepler* mission (Borucki et al. 2010) and *TESS* mission (Ricker et al. 2015). Advances in sophisticated data processing techniques, such as Lares-Martiz et al. (2020), frequencies of low amplitude could be found in the spectrum of HADS as well (Bowman et al. 2021). According to the ratio among the frequencies, the radial modes of HADS could be identified (Petersen 1973), and then by constructing radial frequencies models and comparing the models ratio with the observed ratio, several basic parameters of the star could be obtained, as well as the evolutionary stage (e.g. Xue et al. 2018; Bowman et al. 2021; Daszyńska-Daszkiewicz et al. 2022; Lv et al. 2022). A detailed seismic modeling of SX Phe was performed by Daszyńska-Daszkiewicz et al. (2020), confirmed its post-main sequence evolutionary stage by using a high-precision photometry collected from *TESS* mission. Lv et al. (2021) report a detailed light curve analysis of the *Kepler* target KIC 12602250, and their results show that KIC 12602250 is just pulsating at two radial frequencies. It seems unusual for a low amplitude δ Scuti to have such a clean spectrum, it might be helpful to explore the difference between HADS and normal δ Scuti stars. Therefore, detecting low-amplitude frequencies will enrich the features of light variation and improve the understanding of HADS.

An estimation of the stellar parameters can be made using a scaling relation between the asteroseismic indices and global stellar quantities (e.g. Brown et al. 1991; Kallinger et al. 2010; Coelho et al. 2015; Rodrigues et al. 2017; Hekker 2020). García Hernández et al. (2015), Chen et al. (2019), Rodríguez-Martín et al. (2020) investigated the relationship between the mean density (ρ) and $\Delta\nu$ for δ Scuti stars. The empirical relations between the mean density (ρ) and $\Delta\nu$ for δ Scuti stars were investigated by García Hernández et al. (2015), Chen et al. (2019), Rodríguez-Martín et al. (2020). Due to the δ Scuti pulsations are in the non-asymptotic regime (e.g. Paparó et al. 2016; Mirouh et al. 2019), Suárez et al. (2014) predicted an empirical scaling relation between the large separation and stellar density as $\Delta\nu = 0.78\rho^{0.46}$. Bedding et al. (2020) based on the *TESS* and *Kepler* observations for 60 high-frequency δ Scuti stars obtained a relation as $\Delta\nu = 0.85\sqrt{\rho}$. Hasanzadeh et al. (2021) modified a relation between the large frequency separation and stellar density as $\Delta\nu = (0.76 \pm 0.01)\rho^{0.43\pm0.02}$ for δ Scuti stars (see Fig.13 (Hasanzadeh et al. 2021)). This relation could help us to calculate the stellar density of individual δ Scuti star by analyzing the photometric curve (Huber et al. 2019).

TIC 448892817 (α_{2000}=14^h:26^m:05.899^s, δ_{2000}=+01°:26′:25.727″) is classified as a HADS with a pulsation period of 0.07443 days by Khruslov & Kusakin (2013). Recently, Hasanzadeh et al. (2021) conducted a statistical analysis of the relations between the asteroseismic indices and stellar parameters of δ Scuti stars, TIC 448892817 is included in the statistical work and the asteroseismic indices are given. Combining the pulsation characteristics of HADS one may presume that the mode of highest is a radial mode. Since there is no rotational splitting for radial modes, it provides a very valuable constraint on the models. One would also expect that other radial modes might be present which can be identified from the period ratio in the Petersen diagram (Petersen 1973). Both double radial modes and high frequencies to analyze the stellar asteroseismic indices, making it an excellent target for study. In order to limit the parameters more accurately and attempt to give the evolutionary stages of this star, we downloaded the high-precision photometric data provided by *TESS* and conducted a detailed study. The fundamental parameters of this star are listed in Table 1.

In this paper, Section 2 introduce the observations of TIC 448892817 . The frequency analysis is presented in Section 3. In Section 4, we construct stellar evolution models and make pulsation frequency fitting. A brief discussion and the conclusions are presented in Sections 5 and 6, respectively.

2. OBSERVATIONS AND DATA REDUCTION

The *TESS* Space Telescope (Ricker et al. 2015) observed TIC 448892817 during Sector 5 for 25.6 days from Barycentric Julian Date (BJD) 2458438.06485 to 2458463.70366 in 2 min cadence, and for 26 days from BJD 2458437.99541 to 2459463.99534 in 30-min cadence. All the data were downloaded from TESS Asteroseismic Science Operations Center (TASOC) database [1]. Since the lengths of the two data sets are approximately equal, shorter exposures allow for larger Nyquist detection limits. Therefore, we only used 2-min observations in the subsequent study.

In this work we use the corrected flux and convert it to magnitude. The average value for each sector is then subtracted to obtain the corrected time series. After the above processing, a rectified light curve of 17246 data points with a time span of about 25.6 days was finally obtained. Figure 1 shows a portion of the rectified light curve of TIC 448892817 covering 2.9 days for

[1] TASOC: https://tasoc.dk/search_data/

Table 1. Basic Properties of TIC 448892817

Parameters	TIC 448892817	
Tmag	12.2277	a
Period	0.07443 days	c
$T_{\rm eff}$	7253 K	a
	7798 ± 200 K	b
log g	3.956 dex	a
	4.004 ± 0.021 dex	b
Fe/H	-0.227	a
	-0.149 ± 0.011	b
B	12.28 mag	a
V	12.67 mag	a
J	11.87 mag	a
H	11.67 mag	a
K	11.67 mag	a
Gaia	12.48 mag	a

Note—(a) Parameters from the TASOC. (b) Parameters from the LAMOST. (c) (Khruslov & Kusakin 2013).

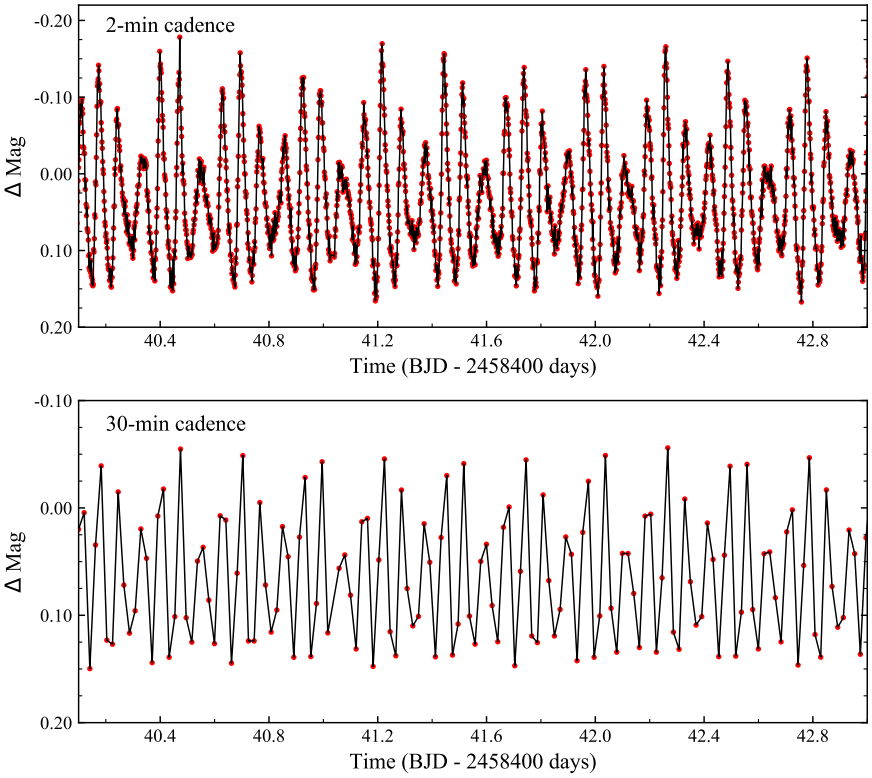

Figure 1. A portion of the long cadence light curve of TIC 448892817 . The amplitude of the light curve is about 0.32 mag.

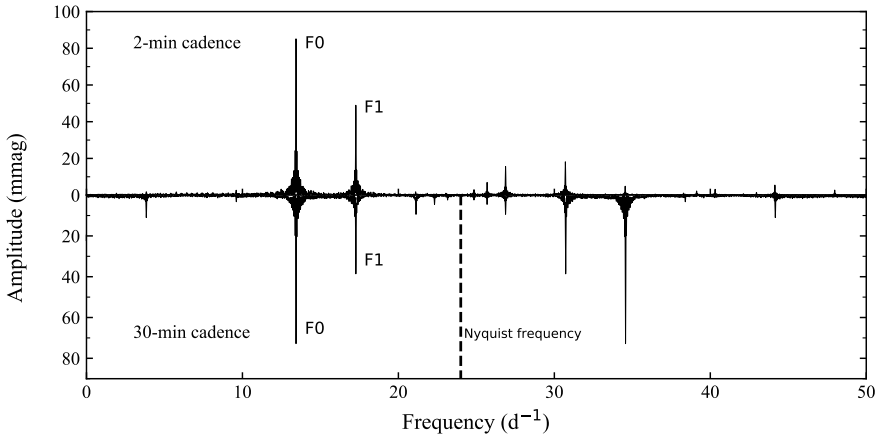

Figure 2. Fourier amplitude spectra and the for the light curve of TIC 448892817 . The top panel shows the independent frequencies F0 and F1 of 2-min cadence. The bottom panel shows the independent frequencies F0 and F1 of 30-min cadence, the dashed line represents Nyquist frequency.

the 2-min and 30-min cadence, respectively. From this figure, the amplitude of 30-min cadence light curve is suppressed due to the longer integration time, resulting in a smaller amplitude than that of the 2-min cadence light curve, and the peak-to-peak amplitude of TIC 448892817 obtained from the rectified light curve is ~0.32 mag, which is typical for HADS stars.

3. FREQUENCY ANALYSIS

To analyze the pulsating behavior of TIC 448892817 , the software PERIOD 04(Lenz & Breger 2005) was utilized during this work. A minimum sampling frequency is set for the Nyquist frequency to prevent alias frequencies (Bowman et al. 2016). The Nyquist frequency of 2-min cadence observations is f_N = 360 d^{-1} (Murphy et al. 2013), well above our limit range of $0 < f <$ 50 d^{-1} for the extracted frequencies. The range of frequencies we extracted covers the typical pulsation interval of δ Scuti stars. In order to distinguish between adjacent closer frequencies in the spectrogram, we use the resolution frequency f_{res} = 1.5 / ΔT (Loumos & Deeming 1978), where ΔT is the length of the data set. When the difference between these two frequencies is larger than the resolution frequency, we assume that these two frequencies have been resolved. The resolution frequency f_{res} = 1.5 / ΔT is 0.0586 d^{-1} for 2-min cadence light curve.

The rectified light curve was fitted with the following formula:

$$m = m_0 + \sum_{i=1}^{N} A_i sin(2\pi(f_i t + \phi_i)), \quad (1)$$

where m_0 is the zero-point, A_i is the amplitude, f_i is the frequency, and ϕ_i is the corresponding phase. In the process of extracting significant frequencies, we usually identify the highest peaks as significant frequencies. The multi-frequency least square fit of the light curve for all detected significant frequencies is then performed using Eq.1 to obtain solutions for all frequencies. The residuals are obtained by subtracting the theoretical light curve constructed by the above solution from the rectification data and continuing the next search using the obtained residuals, repeating the above steps until no significant peaks are found in the spectrum. As the criterion for determining the significance of the detected peaks, we utilize the S/N > 4 suggested by Breger et al. (1993). The frequency uncertainty was determined according to the method proposed by Montgomery & O'donoghue (1999). Figure 2 shows the amplitude spectra for 2-min cadence data and 30-min cadence data, respectively.

Through Fourier transforming the spectrum of TIC 448892817 , a total of 30 frequencies were detected. Stellingwerf (1979) was one of the first papers to predict the period ratios based in theoretical structure models and presented the period ratios of the first two radial modes as: P_1 / P_0 = (0.756 - 787). The two high-amplitude modes of TIC 448892817 have a period ratio of 0.778 identifying them as the fundamental and first overtone radial modes (Breger & Montgomery 2000). Combination frequencies were identified by searching for linear sum and difference frequencies, nν_i ± mν_j, with the Loumos & Deeming (1978) criterion as a tolerance and assuming that the highest-amplitude peaks within a combination family are the real pulsation mode frequencies (Kurtz et al. 2015). Therefore, the fundamental frequency f_1 with 'F0', first overtone f_2 with 'F1' and the combination frequencies (i.e. f_3, f_5, f_8...f_{13}) and harmonics frequencies (i.e. f_4, f_6, f_7) of the two radial modes are listed in Table 2. The remaining 17

Table 2. The radial pulsation mode frequencies in SC data of TIC 448892817 .

f_i	Frequency (d^{-1})	Amplitude (mmag)	Phase (rad)	S/N	Comment
1	13.43538 ± 0.00002	84.711 ± 0.085	0.8868 ± 0.0002	224.5	F0
2	17.27007 ± 0.00004	48.527 ± 0.085	0.3028 ± 0.0003	139.6	F1
3	30.70536 ± 0.00010	18.154 ± 0.085	0.1961 ± 0.0008	124.3	F0+F1
4	26.87060 ± 0.00012	15.586 ± 0.085	0.8888 ± 0.0009	89.6	2F0
5	44.14062 ± 0.00033	5.511 ± 0.085	0.1429 ± 0.0025	53.7	2F0+F1
6	34.53957 ± 0.00038	4.814 ± 0.085	0.3409 ± 0.0028	36.4	2F1
7	40.30572 ± 0.00059	3.136 ± 0.085	0.0483 ± 0.0044	26.4	3F0
8	47.97518 ± 0.00066	2.804 ± 0.085	0.7588 ± 0.0049	34.3	F0+2F1
9	9.59390 ± 0.00080	2.297 ± 0.085	0.4983 ± 0.0059	5.7	2F0-F1
10	21.10437 ± 0.00093	1.992 ± 0.085	0.4386 ± 0.0069	13.1	2F1-F0
11	3.83563 ± 0.00096	1.924 ± 0.085	0.3154 ± 0.0071	4.5	F1-F0
12	23.03251 ± 0.00196	0.941 ± 0.085	0.6518 ± 0.0145	6.9	3F0-F1
13	24.90467 ± 0.00188	0.979 ± 0.085	0.2767 ± 0.0139	6.6	3F1-2F0

Note—Among these frequencies, 2 peaks are independent frequencies, others are harmonic or combinations (denoted by f_i).

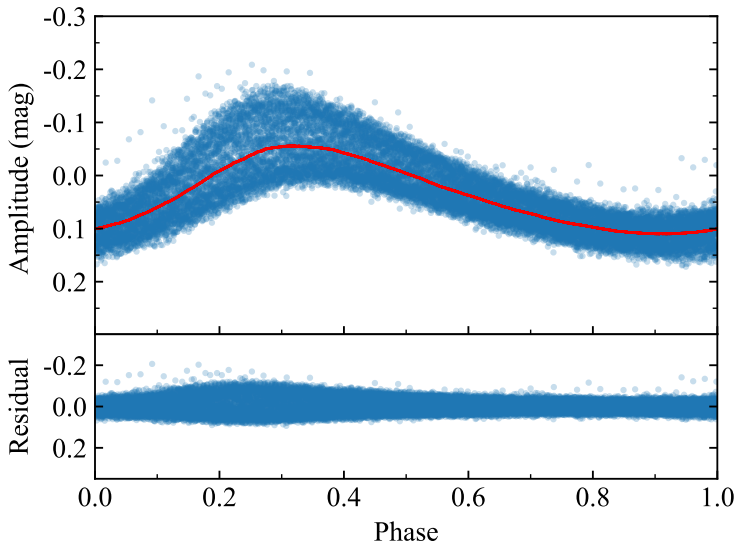

Figure 3. Phase diagram of TIC 448892817 , folded by the fundamental frequency F0 = 13.43538(2)) d^{-1}. The phase diagram shows that the light variation has a tendency to climb rapidly and fall slowly, which is typical of HADS.

frequencies are non-radial pulsation frequencies listed in Table A. Figure 3 shows the phase diagram of TIC 448892817 , folded by the fundamental frequency F0 = 13.43538(2) d^{-1}. The phase diagram shows that the light variation has a tendency to climb rapidly and fall slowly, which is typical of HADS.

4. STELLAR MODEL AND FITTING RESULTS

Table 3. The parameters of the models that reproduce exactly the observed dominant frequency f1 as the radial fundamental mode (l = 0) and closely match the observed frequency f2 as the radial first overtone (l = 0). All models have an initial hydrogen abundance of X_0 = 0.70, mixing length parameter α = 1.9. The mass, Z, effective temperature, luminosity, surface gravity, age, theoretical frequency of fundamental, first overtone radial modes and their ratios of best-fitting models are provided.

M ($M_\odot$)	Z	log $T_{\rm eff}$	log($L/L_\odot$)	log g	Age (10^9 years)	f_1 (d^{-1})	f_2 (d^{-1})	f_1 / f_2	$\frac{dP_0}{dt}$ ($\times 10^{-8}$)
1.63	0.0009	3.9865	1.5371	4.0124	1.0675	13.4376	17.2691	0.7781	1.28
1.64	0.0009	3.9882	1.5456	4.0135	1.0467	13.4378	17.2699	0.7781	1.25
1.67	0.001	3.9906	1.5604	4.0163	0.9905	13.4286	17.2652	0.7778	1.25
1.63	0.006	3.8987	1.1780	4.0203	1.1690	13.4104	17.2866	0.7758	-0.07
1.65	0.006	3.9007	1.1894	4.0221	1.1083	13.4086	17.2778	0.7761	0.09
1.67	0.006	3.9107	1.2333	4.0236	1.1081	13.4111	17.2905	0.7756	-0.55
1.68	0.006	3.9064	1.2177	4.0246	1.0437	13.4063	17.2755	0.7760	0.12
1.74	0.006	3.9183	1.2752	4.0299	0.9328	13.4104	17.2769	0.7762	0.16

We constructed a grid of evolutionary models of stars and calculated their corresponding adiabatic frequencies using the Modules for Experiments in Stellar Astrophysics (MESA v11701; Paxton et al. 2011, 2013, 2015, 2018, 2019) and the stellar oscillation code GYRE (Townsend & Teitler 2013). Our theoretical models are constructed on basis of the OPAL opacity table GS98 (Grevesse & Sauval 1998) series. The classical mixing length theory of (Böhm-Vitense 1958) with α = 1.90 (Paxton et al. 2013) is used in the convective region. Effects of element diffusion, convective overshooting, and rotation are not included in our calculations.

In our calculations, we fix the mixing-length parameter α = 1.90 and set the initial helium fraction $Y = 0.249 + 1.33Z$ (Li et al. 2018) as a function of the metallicity Z. There are large uncertainties associated with determining the metallicity with a low-resolution spectrum from LAMOST (Cui et al. 2012). Therefore, we chose to survey a range of models with different metallicities between $0.002 \leq Z \leq 0.030$ in steps of 0.002, and determine the best-fitting mass and age. The stellar mass M varies from 1.50 $M_\odot$ to 2.80 $M_\odot$ with a step of 0.01 $M_\odot$. Each model in the above grid was evolved from the zero-age MS to the post-MS stage with T_{eff} = 5600 K.

Since $TESS$ data are of exceptionally high quality, the two dominant pulsation mode frequencies and their frequency ratio are known to a very high precision. The high amplitudes of the pulsation modes and their frequency ratio indicate that they are likely the fundamental and first overtone radial modes, so a sensible method to model TIC 448892817 is by using Petersen diagrams. The frequency and frequency ratio of radial modes depend primarily on the mass, age, evolutionary stage, and metallicity. The Petersen diagrams therefor provides a useful diagnostic method in terms of constraining these parameters of radial pulsators (see e.g. Petersen 1973; Petersen & Christensen-Dalsgaard 1996; Daszyńska-Daszkiewicz et al. 2020; Bowman et al. 2021; Lv et al. 2022). we provide the best-fitting mass, Z, effective temperature, luminosity, surface gravity, age, theoretical frequency of fundamental, first overtone radial modes and their ratios are listed in Table 3. The ratio P_1 / P_0 is mostly in the narrow range $0.77 < P_1 / P_0 < 0.78$. Lower metallicity has the effect of shifting period ratios towards slightly higher values for the same mass (Balona et al. 2012). As can be seen from the table, the model ratios are closer to the observed values for models with lower metal abundances. Since these models with low metallicity give too high temperatures that are significantly larger than the temperature range of δ Scuti and the observed values from LAMOST. Moreover, the metallicity obtained from LAMOST were also significantly greater than 0.001. In Figure 4 we showed the evolutionary tracks of the models in Table 3 except for the low metallicity models from the zero-age MS to the post-MS stage in order to better understand the evolution of TIC 448892817 . The color lines represent different combinations of metallicity Z and mass M. The crosses mark the minimum χ^2 ((Chen et al. 2019), i.e. Equation (5), χ^2 method) for each specific model. In order to be in line with the derived value of T_{eff} given by $TESS$ (7253 K) and LAMOST low resolution spectrum (7798 ± 200 K), models with a broader range of temperature between 7000 and 8500 K were adopted. We note all these models suggest that TIC 448892817 is located on the close to the first turn-off of the main sequence.

5. DISCUSSION

As can be seen from Table 3, The frequency ratios f_1/f_2 obtained by the model are a little smaller than those obtained by observation. HADS typically has a low rotational velocities with $v \sin i < 30$ km s^{-1}, Suárez et al. (2007) propose that the effect

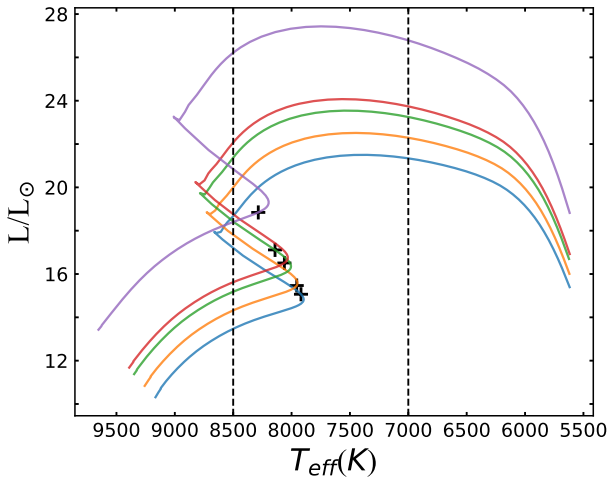

Figure 4. Evolutionary tracks from the zero-age MS to the post-MS for the 5 candidate models except for the low metallicity models, as listed in Table 3. The plus sign mark the minimum χ^2 for each specific model by fitting the calculated f_1 and f_2 with the observed values. The two vertical dotted lines mark Teff at 7000 K and 8500 K, respectively.

Table 4. The stellar parameters are collected from Hasanzadeh et al. (2021) and the best model derived in this paper, respectively.

	Mass ($M_\odot$)	Radius ($R_\odot$)	log g	log($L/L_\odot$)
Hasanzadeh et al. (2021)	1.63±0.27	2.22±0.15	3.96±0.1	1.091±0.181
This paper	$1.68^{+0.06}_{-0.05}$	$2.08^{+0.02}_{-0.02}$	$4.0241^{+0.0059}_{-0.0038}$	$1.218^{+0.057}_{-0.040}$

of near-degeneracy on the frequencies becomes very important for rotational velocities larger than about 15−20 km s^{-1}. Suárez et al. (2006) concludes that the period ratio f_1/f_2 increases with the increase of the rotation velocities by calculated the period ratios for different rotational velocities (Rotational Petersen Diagrams) and metallicities, and then compared with classic non-rotating ones. Even for slow rotators, the effect of rotation on the period ratio also can be significant (Suárez et al. 2007). Thus, the observed ratio is larger than the model, which may be caused by the rotation of the star.

The degeneracy between mass and age cannot generally be broken by fitting the two pulsation modes alone (Bowman et al. 2021). Hence one needs additional information, such as fitting a third mode or including spectroscopic constraints, to constrain the age of a star. The target is an excellent object of study since it has not only two confirmed radial modes but also an asymptotic region in the high frequency, allowing us to obtain an asteroseismic indices. The models result we obtained could be verified by comparing the stellar density deduced from the asteroseismic indices and obtained from the best fitting models.

Hasanzadeh et al. (2021) investigate the relationship between the asteroseismic indices and the physical quantities of 438 δ Scuti stars observed by the *TESS* mission at 26 sectors. They used an empirical relation and a 2D autocorrelation method, derived the asteroseismic indices of these stars. Table 4 shows the parameters from Hasanzadeh et al. (2021) and the average of the parameters obtained by our best models. As the result shows, the parameters we obtained are basically the same. And the basic parameters we obtained from models is close to the spectroscopically measured value. Hasanzadeh et al. (2021) gives the asteroseismic indices ν_{max} and $\Delta\nu$ for TIC 448892817 as 35.42 d^{-1} and 3.85 d^{-1}, respectively. Since this star has many combination frequencies and harmonics frequencies of two radial frequencies in the high frequency region, so the $\Delta\nu$ derived by Hasanzadeh et al. (2021) may be inaccurate. We used the ν_{max} given by Hasanzadeh et al. (2021) to calculate the $\Delta\nu$ of this star by using the relationship $\Delta\nu = (0.49 \pm 0.12)\nu_{max}{}^{(0.68\pm0.07)}$ (Hasanzadeh et al. 2021), the result is $\Delta\nu = 5.54^{+3.31}_{-2.28}$ d^{-1}, and after using the relationship $\Delta\nu = 0.85\sqrt{\rho}$ derive the density (Bedding et al. 2020), then the density of TIC 448892817 is obtained $\rho = 0.226^{+0.57}_{-0.118}$ g/cm^3, which is basically consistent with the density obtained by our models, the density calculated by the models is 0.262 g/cm^3.

When compared with another five HADS stars (see Table 12 in (Xue et al. 2018)), we note TIC 448892817 has the shortest $P0$. Using the basic pulsation relation $P\sqrt{\bar{\rho}/\rho_\odot} = Q$ (P is the period and Q is the pulsation constant). Then this leads to the largest $\bar{\rho}$ for TIC 448892817 among the six HADS, revealing that TIC 448892817 is still at an earlier stage than the others. Our result

is consistent with the tendency derived by Xue et al. (2018), that the lower the fundamental frequency is, the later the star would have evolved into (also see Figure 9 in (Xue et al. 2018)). Indicates that TIC 448892817 is close to entering the first turn-off of the main sequence.

Although we compare the model results with the stellar parameters calculated by the asteroseismic indices and the results were generally consistent, We still suggest high-resolution spectra is highly desired in the future, which would provide other parameters, and further narrow down the parameter space of this star.

6. SUMMARY

We have analyzed the pulsating behavior of TIC 448892817 using high-precision photometric observations from $TESS$ mission, and 30 significant frequencies are detected, while two of them are independent frequencies, i.e. F0 = 13.43538(2) d^{-1}, F1 = 17.27007(4) d^{-1}. The ratio of f_1 / f_2 is measured to be 0.7780, suggesting that this target is a high amplitude double-mode δ Scuti star. Nearly all the light variation is due to these two modes and their combination frequencies, but several other frequencies of very low amplitude are also present.

The stellar evolutionary models were constructed with different mass M and metallicity Z using MESA. The frequency ratios f_1/f_2 obtained by the model are a little smaller than those obtained by observation. It could be caused by the rotation of the star. The parameters obtained from the model agree well with the LAMOST spectra and the parameters derived by asteroseismic indices. The best model shows that TIC 448892817 is close to entering the first turn-off of the main sequence.

we still suggest that high-resolution spectroscopic observations of TIC 448892817 would not only help to accurately determine the effective temperature and metallicities, but also provide other parameters such as rotation rate, radial velocity, thus further narrowing the parameter space of this star. we have shown in this work that $TESS$ data can be provide a real-time picture of stellar evolution, thus opening a window to the development of ultra-precise stellar models.

ACKNOWLEDGMENTS

This research is supported by the National Natural Science Foundation of China (grant No. U2031209). We would like to thank the $TESS$ science team for providing such excellent data. The Large Sky Area Multi-Object Fiber Spectroscopic Telescope (LAMOST) is a National Major Scientific Project built by the Chinese Academy of Sciences. Funding for the project has been provided by the National Development and Reform Commission. LAMOST is operated and managed by the National Astronomical Observatories, Chinese Academy of Sciences.

APPENDIX

The additional independent non-radial pulsation mode frequencies identified in the 2 min cadence *TESS* data of TIC 448892817 are provided in Tables A.

Table A. Additional independent frequencies extracted from the 25.6 days 2 min cadence *TESS* data of TIC 448892817 (i.e. F0, F1 and all their significant combinations and harmonics frequencies have been removed).

f_{Si}	Frequency (d^{-1})	Amplitude (mmag)	Phase (rad)	S/N
1	25.68703 ± 0.00026	6.997 ± 0.085	0.8301 ± 0.0020	25.6
2	24.84656 ± 0.00060	3.050 ± 0.085	0.3317 ± 0.0045	19.2
3	39.12086 ± 0.00075	2.447 ± 0.085	0.8321 ± 0.0056	16.6
4	42.95601 ± 0.00112	1.648 ± 0.085	0.5990 ± 0.0083	12.6
5	38.28176 ± 0.00172	1.072 ± 0.085	0.3398 ± 0.0127	9.0
6	29.51877 ± 0.00224	0.822 ± 0.085	0.4957 ± 0.0166	6.5
7	42.12076 ± 0.00223	0.825 ± 0.085	0.5525 ± 0.0165	7.8
8	21.85071 ± 0.00233	0.790 ± 0.085	0.8115 ± 0.0173	6.1
9	26.13133 ± 0.00257	0.718 ± 0.085	0.3783 ± 0.0190	6.0
10	24.63945 ± 0.00259	0.712 ± 0.085	0.4027 ± 0.0192	5.7
11	33.25919 ± 0.00297	0.622 ± 0.085	0.9505 ± 0.0220	5.5
12	40.87850 ± 0.00320	0.575 ± 0.085	0.0074 ± 0.0237	5.9
13	35.28737 ± 0.00350	0.526 ± 0.085	0.7689 ± 0.0259	4.3
14	36.47112 ± 0.00366	0.504 ± 0.085	0.7569 ± 0.0271	4.3
15	38.37448 ± 0.00384	0.480 ± 0.085	0.6088 ± 0.0284	4.4
16	22.28560 ± 0.00390	0.473 ± 0.085	0.0744 ± 0.0288	4.4
17	33.13828 ± 0.00433	0.424 ± 0.085	0.0796 ± 0.0320	4.1

REFERENCES

Aerts, C., Christensen-Dalsgaard, J., & Kurtz, D. W. 2010, Asteroseismology, Astronomy and Astrophysics Library. ISBN 978-1-4020-5178-4. Springer Science+Business Media B.V., 2010, p.

Aerts, C. 2021, Reviews of Modern Physics, 93, 015001. doi:10.1103/RevModPhys.93.015001

Auvergne, M., Bodin, P., Boisnard, L., et al. 2009, A&A, 506, 411. doi:10.1051/0004-6361/200810860

Balona, L. A., Lenz, P., Antoci, V., et al. 2012, MNRAS, 419, 3028. doi:10.1111/j.1365-2966.2011.19939.x

Bedding, T. R., Murphy, S. J., Hey, D. R., et al. 2020, Nature, 581, 147. doi:10.1038/s41586-020-2226-8

Bowman, D. M., Kurtz, D. W., Breger, M., et al. 2016, MNRAS, 460, 1970. doi:10.1093/mnras/stw1153

Bowman, D. M., Hermans, J., Daszyńska-Daszkiewicz, J., et al. 2021, MNRAS, 504, 4039. doi:10.1093/mnras/stab1124

Borucki, W. J., Koch, D., Basri, G., et al. 2010, Science, 327, 977. doi:10.1126/science.1185402

Böhm-Vitense, E. 1958, ZA, 46, 108

Breger, M., Stich, J., Garrido, R., et al. 1993, A&A, 271, 482

Breger, M. & Montgomery, M. 2000, Delta Scuti and Related Stars, 210

Breger, M. 2000, Delta Scuti and Related Stars, 210, 3

Brown, T. M., Gilliland, R. L., Noyes, R. W., et al. 1991, ApJ, 368, 599. doi:10.1086/169725

Brown, T. M. & Gilliland, R. L. 1994, ARA&A, 32, 37. doi:10.1146/annurev.aa.32.090194.000345

Catelan, M. & Smith, H. A. 2015, Pulsating Stars (Wiley-VCH), 2015

Campante, T. L., Schofield, M., Kuszlewicz, J. S., et al. 2016, ApJ, 830, 138. doi:10.3847/0004-637X/830/2/138

Chen, X., Li, Y., & Zhang, X. 2019, ApJ, 887, 253. doi:10.3847/1538-4357/ab585b

Coelho, H. R., Chaplin, W. J., Basu, S., et al. 2015, MNRAS, 451, 3011. doi:10.1093/mnras/stv1175

Cui, X.-Q., Zhao, Y.-H., Chu, Y.-Q., et al. 2012, Research in Astronomy and Astrophysics, 12, 1197. doi:10.1088/1674-4527/12/9/003

Daszyńska-Daszkiewicz, J., Pamyatnykh, A. A., Walczak, P., et al. 2020, MNRAS, 499, 3034. doi:10.1093/mnras/staa3056

Daszyńska-Daszkiewicz, J., Walczak, P., Pamyatnykh, A. A., et al. 2022, MNRAS, 512, 3551. doi:10.1093/mnras/stac646

Dupret, M.-A., Thoul, A., Scuflaire, R., et al. 2004, A&A, 415, 251. doi:10.1051/0004-6361:20034143

García Hernández, A., Martín-Ruiz, S., Monteiro, M. J. P. F. G., et al. 2015, ApJL, 811, L29. doi:10.1088/2041-8205/811/2/L29

García, R. A. & Ballot, J. 2019, Living Reviews in Solar Physics, 16, 4. doi:10.1007/s41116-019-0020-1

Gilliland, R. L., Brown, T. M., Christensen-Dalsgaard, J., et al. 2010, PASP, 122, 131. doi:10.1086/650399

Grevesse, N. & Sauval, A. J. 1998, SSRv, 85, 161. doi:10.1023/A:1005161325181

Guo, Z., Fuller, J., Shporer, A., et al. 2019, ApJ, 885, 46. doi:10.3847/1538-4357/ab41f6

Hasanzadeh, A., Safari, H., & Ghasemi, H. 2021, MNRAS, 505, 1476. doi:10.1093/mnras/stab1411

Hekker, S. 2020, Frontiers in Astronomy and Space Sciences, 7, 3. doi:10.3389/fspas.2020.00003

Huber, D., Chaplin, W. J., Chontos, A., et al. 2019, AJ, 157, 245. doi:10.3847/1538-3881/ab1488

Kallinger, T., Mosser, B., Hekker, S., et al. 2010, A&A, 522, A1. doi:10.1051/0004-6361/201015263

Khruslov, A. V. & Kusakin, A. V. 2013, Peremennye Zvezdy, 33, 6

Koch, D. G., Borucki, W. J., Basri, G., et al. 2010, ApJL, 713, L79. doi:10.1088/2041-8205/713/2/L79

Kurtz, D. W., Shibahashi, H., Murphy, S. J., et al. 2015, MNRAS, 450, 3015. doi:10.1093/mnras/stv868

Lares-Martiz, M., Garrido, R., & Pascual-Granado, J. 2020, MNRAS, 498, 1194. doi:10.1093/mnras/staa2256

Lenz P., Breger M. 2005, CoAst, 146, 53

Li, T., Bedding, T. R., Huber, D., et al. 2018, MNRAS, 475, 981. doi:10.1093/mnras/stx3079

Lopez de Coca, P., Rolland, A., Rodriguez, E., et al. 1990, A&AS, 83, 51

Loumos, G. L. & Deeming, T. J. 1978, Ap&SS, 56, 285. doi:10.1007/BF01879560

Lv, C.-L., Esamdin, A., Liu, J.-H., et al. 2021, Research in Astronomy and Astrophysics, 21, 224. doi:10.1088/1674-4527/21/9/224

Lv, C., Esamdin, A., Zeng, X., et al. 2021, AJ, 162, 48. doi:10.3847/1538-3881/ac082b

Lv, C., Esamdin, A., Pascual-Granado, J., et al. 2022, arXiv:2205.00571

McNamara D. H., 2000, in Delta Scuti and Related Stars,. M. Breger, & M. H. Montgomery, ASP Conf.Ser., 210, 373

Mirouh, G. M., Angelou, G. C., Reese, D. R., et al. 2019, MNRAS, 483, L28. doi:10.1093/mnrasl/sly212

Miszuda, A., Szewczuk, W., & Daszyńska-Daszkiewicz, J. 2021, MNRAS, 505, 3206. doi:10.1093/mnras/stab1597

Montgomery M. H., & O'donoghue D., 1999, Delta Scuti Star Newsletter, 13, 28

Mombarg, J. S. G., Van Reeth, T., & Aerts, C. 2021, A&A, 650, A58. doi:10.1051/0004-6361/202039543

Murphy, S. J., Shibahashi, H., & Kurtz, D. W. 2013, MNRAS, 430, 2986. doi:10.1093/mnras/stt105

Murphy, S. J., Bedding, T. R., Niemczura, E., et al. 2015, MNRAS, 447, 3948. doi:10.1093/mnras/stu2749

Murphy, S. J., Saio, H., Takada-Hidai, M., et al. 2020, MNRAS, 498, 4272. doi:10.1093/mnras/staa2667
Niu, J.-S., Fu, J.-N., Li, Y., et al. 2017, MNRAS, 467, 3122
Paparó, M., Benkő, J. M., Hareter, M., et al. 2016, ApJS, 224, 41. doi:10.3847/0067-0049/224/2/41
Paxton, B., Bildsten, L., Dotter, A., et al. 2011, ApJS, 192, 3. doi:10.1088/0067-0049/192/1/3
Paxton, B., Cantiello, M., Arras, P., et al. 2013, ApJS, 208, 4. doi:10.1088/0067-0049/208/1/4
Paxton, B., Marchant, P., Schwab, J., et al. 2015, ApJS, 220, 15. doi:10.1088/0067-0049/220/1/15
Paxton, B., Schwab, J., Bauer, E. B., et al. 2018, ApJS, 234, 34. doi:10.3847/1538-4365/aaa5a8
Paxton, B., Smolec, R., Schwab, J., et al. 2019, ApJS, 243, 10. doi:10.3847/1538-4365/ab2241
Petersen, J. O. 1973, A&A, 27, 89
Petersen, J. O. & Christensen-Dalsgaard, J. 1996, A&A, 312, 463
Ricker, G. R., Winn, J. N., Vanderspek, R., et al. 2015, Journal of Astronomical Telescopes, Instruments, and Systems, 1, 014003. doi:10.1117/1.JATIS.1.1.014003
Rodríguez, E. & Breger, M. 2001, A&A, 366, 178. doi:10.1051/0004-6361:20000205
Rodríguez-Martín, J. E., García Hernández, A., Suárez, J. C., et al. 2020, MNRAS, 498, 1700. doi:10.1093/mnras/staa2378
Rodrigues, T. S., Bossini, D., Miglio, A., et al. 2017, MNRAS, 467, 1433. doi:10.1093/mnras/stx120
Saio, H., Kurtz, D. W., Takata, M., et al. 2015, MNRAS, 447, 3264. doi:10.1093/mnras/stu2696
Stellingwerf, R. F. 1979, ApJ, 227, 935
Stello, D., Saunders, N., Grunblatt, S., et al. 2022, MNRAS. doi:10.1093/mnras/stac414
Suárez, J. C., Garrido, R., & Goupil, M. J. 2006, A&A, 447, 649. doi:10.1051/0004-6361:20053866
Suárez, J. C., Garrido, R., & Moya, A. 2007, A&A, 474, 961. doi:10.1051/0004-6361:20077647
Suárez, J. C., García Hernández, A., Moya, A., et al. 2014, A&A, 563, A7. doi:10.1051/0004-6361/201322270
Thomson-Paressant, K., Neiner, C., Zwintz, K., et al. 2021, MNRAS, 500, 1992. doi:10.1093/mnras/staa3442
Townsend, R. H. D. & Teitler, S. A. 2013, MNRAS, 435, 3406. doi:10.1093/mnras/stt1533
Uytterhoeven, K., Moya, A., Grigahcène, A., et al. 2011, A&A, 534, A125. doi:10.1051/0004-6361/201117368
Viskum, M., Kjeldsen, H., Bedding, T. R., et al. 1998, A&A, 335, 549
Walker, G., Matthews, J., Kuschnig, R., et al. 2003, PASP, 115, 1023. doi:10.1086/377358
Xue, H.-F., Fu, J.-N., Fox-Machado, L., et al. 2018, ApJ, 861, 96. doi:10.3847/1538-4357/aac9c5
Yang, T.-Z., Esamdin, A., Fu, J.-N., et al. 2018, Research in Astronomy and Astrophysics, 18, 002
Yang, X. H., Fu, J. N., & Zha, Q. 2012, AJ, 144, 92
Yu, J., Huber, D., Bedding, T. R., et al. 2018, ApJS, 236, 42. doi:10.3847/1538-4365/aaaf7